Journal of Structural Geology, Vol. 6, No. 1/2, pp. 33 to 38, 1984
Printed in Great Britain

0191-8141/84 $03.00 + 0.00
Pergamon Press Ltd.

Development of planar and linear fabrics in Dauphinois shales and slates (French Alps) studied by magnetic anisotropy and its mineralogical control

P. ROCHETTE

I.R.I.G.M. ERA603, B.P. 68, 38402 St Martin d'Heres Cedex, France

and

P. VIALON

Laboratoire Louis Neel, C.N.R.S., 38042 Grenoble Cedex, France

(*Accepted in revised form* 28 *June* 1983)

Abstract—The progressive development of planar and linear fabrics due to Alpine deformation in Dogger calcareous shales has been studied in the Dauphinois zone of the French Alps, using measurements of the anisotropy of magnetic susceptibility. The axes and shapes of magnetic ellipsoids and petrofabrics show good qualitative correlation through a series of different fabric types from a sedimentary to a highly deformed one.

Together with various petrological techniques, magnetization measurements in a variable field (up to 5 T) and under variable temperature with a cryogenic magnetometer, were used to achieve a complete analysis of the magnetic mineralogy with its dia-, para- and ferromagnetic (*s.l.*) contributions. The effects on the anisotropy of the complex mineralogy and various geological processes including pressure-solution, metamorphism and weathering, are discussed.

INTRODUCTION

IN THE Dauphinois zone of the French Alps, described by Ramsay (1963), along the northwest side of the external crystalline massifs lies a continuous belt of Lias and Dogger calcareous shales (Fig. 1). These weak layers form a privileged shearing zone and were deformed during the Alpine thrusting and the northwestward transport of the upper units, sub-Alpine massifs and Prealps. This deformation has led to a spaced regional cleavage dipping to the southeast and to folds verging to the northwest. As can be seen in the Helvetic and Prealps nappes, the deformation has a clear lateral gradient from the southwest to the northeast. Illite crystallinity and fluid inclusion temperatures indicate a correlative increase of metamorphism, reaching the epizone in the Megève region (Zwart 1973) where paragonite has been observed. In the eastern sedimentary cover of the crystalline massifs (sites K and L in Fig. 1) deformation and metamorphism are even higher (Bernard *et al.* 1977, Gratier & Vialon 1980). It is in this framework that the relationships between magnetic properties and petrofabrics have been studied.

PETROFABRICS

Twelve sites were sampled in the homogeneous series of dark calcareous Dogger shales (Fig. 1). Optical examinations and X-ray diffractometry indicate the following mineralogy: calcite, quartz, chlorite, illite and pyrite. In the most metamorphosed sites, illite is replaced by paragonite or muscovite. In some weathered samples iron oxyhydroxydes become abundant within the cleavage planes. The bedding is marked by a decimetric and millimetric compositional layering.

The beginning of deformation took place principally through a mechanism of pressure-solution, indeed calcite and quartz were dissolved at the level of cleavage foliae and grew again in tension gashes. The cleavage foliae correspond to an iron-enrichment zone where

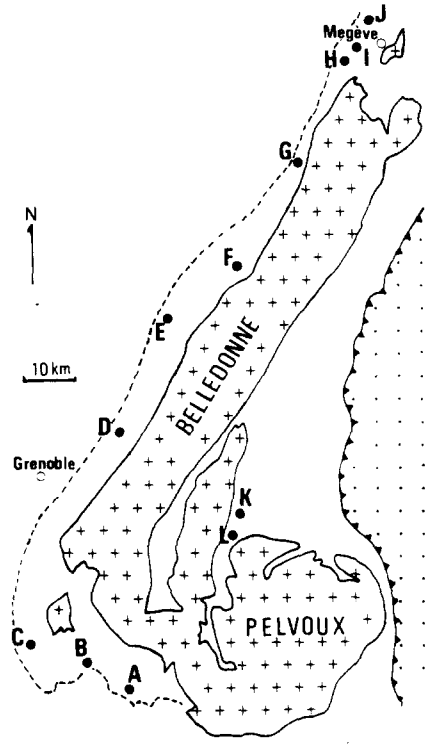

Fig. 1. Simplified map of the Dauphinois zone (French Alps) showing the external crystalline massifs, the western upper limit of Dogger outcrops (dashed line) and the location of the sites labeled from A to L. The Penninic zone is shown stippled.

phyllosilicates and opaque grains accumulated more or less passively (cf. Gratier 1982, Rochette 1983). The increase in deformation results in a densification of the cleavage foliae, a decrease in the angle between the bedding and cleavage planes and the appearance of a significant amount of grain rotation and oriented recrystallization. In the Megève region (sites H, I and J) a northwestward stretching lineation due to the transport appears, superposed on the NE-trending bedding-cleavage intersection lineation (Pijolat *et al.* 1981). A westward stretching lineation is strongly developed in the eastern sites, K and L.

The sequence of fabric types described by Ramsay (1982) is observed: beginning with an oblate sedimentary fabric (sites A and B), the superposition of a cleavage oblique to the bedding gives a prolate intersection fabric or pencil structure (sites C, D, F and G), then the oblate tectonic fabric parallel to the cleavage predominates (sites E, H, I, J and K); finally the stretching lineation gives a prolate fabric, while the cleavage has a less constant attitude (site L).

MAGNETIC FABRIC

Measurement and representation

Extensive measurements of the anisotropy of low-field susceptibility were carried out using a Digico anisotropy delineator. The direction and magnitude of the three principal axes of the susceptibility ellipsoid ($K_1 > K_2 > K_3$) were thus determined. To quantify the intensity of the anisotropy the parameter P (degree of anisotropy) is used, where:

$$P = \frac{K_1}{K_3}. \qquad (1)$$

The symmetry of the anisotropy ellipsoid is described by the parameter V (Coward & Whalley 1979, Jelinek 1981), where

$$V = \frac{2k_2 - (k_1 + k_3)}{k_1 - k_3} \text{ and } k_i = \log_e K_i. \qquad (2)$$

The value of V is 0 for a plane anisotropy ellipsoid, +1 for a uniaxial oblate ellipsoid, and −1 for a uniaxial prolate ellipsoid.

Magnetic mineralogy

The anisotropy of low-field susceptibility, K_0, can be due to the preferred orientation of various magnetically anisotropic minerals with dia-, para-, antiferro- or ferromagnetic (*s.l.*) behaviours (Owens & Bamford 1976, Hrouda 1982). To understand the relation between the petrofabric and the magnetic fabric, a close control of the magnetic mineralogy is necessary. In fact, especially in rocks with low values of K_0, there is generally more than one mineral which contributes to the value and anisotropy of K_0, as shown by Coward & Whalley (1979) using magnetic measurements in a variable field up to 0.68 T.

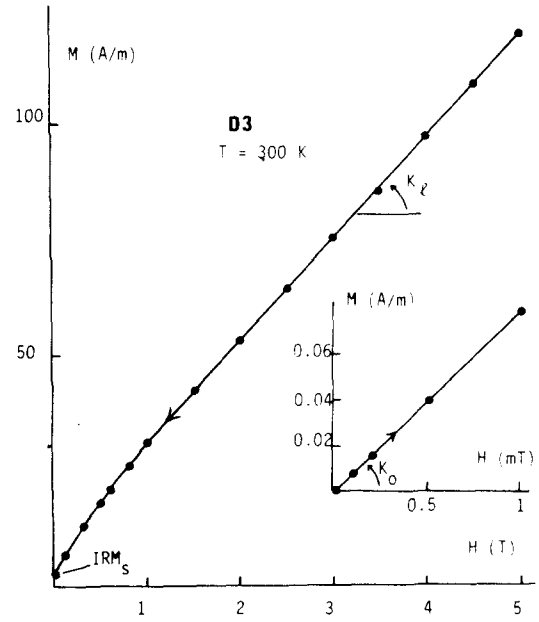

Fig. 2. Induced magnetization curve in high and low fields measured in the cryogenic magnetometer at room temperature for sample D3.

In the present study a complete quantitative analysis of K_0 has been performed on several selected samples using magnetization measurements in a variable field up to 5 T and under variable temperature, with a cryogenic S.H.E. magnetometer. This apparatus can measure 12 mm-high cubic samples with a noise level of less than 10^{-4} A/m. At room temperature the magnetization curve of a sample shows two parts (Fig. 2): one, which is linear at any field strength, is the sum of the para-, dia- and antiferromagnetic contributions. All these minerals form the matrix, characterized by the high-field susceptibility, K_f, and in which are dispersed few ferromagnetic grains responsible for the saturating part of the curve. The ferromagnetic (*s.l.*) contribution is characterized by the isothermal remanent magnetization at saturation, IRM_s, and by a ferromagnetic low field susceptibility, K_f, derived from K_0 measured between 0 and 1 mT by the subtraction of K_f. This operation implies that the ferromagnetic grains are saturated in the fields used to measure K_f: between 3 and 5 T. For diamagnetic materials and paramagnetic salts it has been verified that K_0 and K_f are equal. Paramagnetic salts were also used to calibrate the value of K_0 between the Digico A.C. bridge and the cryogenic magnetometer.

The matrix susceptibility K_f, ranging from 20 to 180 10^{-6} SI, can be further analysed through its thermal variation (Rochette *et al.* 1983). For several samples it has been possible to fit this variation with the following law

$$K_f = C/(T - \theta) + D, \qquad (3)$$

where C, θ and D are constants and T is the absolute temperature. It separates a predominant paramagnetic term, $C/(T - \theta)$, from a diamagnetic term, D, as shown for sample L8 in Fig. 3. For five samples, a mean diamagnetic susceptibility of -15×10^{-6} is observed. This value, intermediate between the susceptibilities of calcite and quartz, -13 and -17×10^{-6} (Carmichael

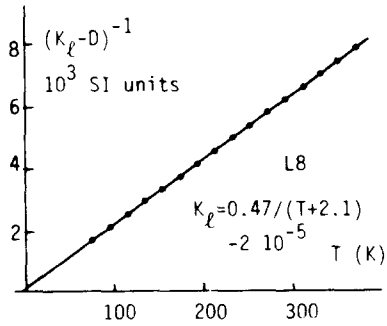

Fig. 3. Linear regression plot of $(K_l - D)^{-1}$ vs T (absolute temperature) between 70 and 370 K for sample L8. *K_l is the high-field susceptibility and D* the best-fitted diamagnetic term.

1982) is quite correct for a calcareous shale matrix, although no data are available for the diamagnetic susceptibility of phyllosilicates.

The paramagnetic minerals in sample L8 have been identified by Mössbauer spectroscopy coupled with X-ray diffractometry. The Mössbauer spectrum recorded at room temperature has been interpreted as due to the superposition of three doublets (Fig. 4). The Mössbauer parameters of these doublets (see Table 1) are in good agreement with those already observed for iron in pyrite (Evans *et al.* 1982) and for Fe^{2+} in chlorite and muscovite (Heller-Kallai & Rozenson 1981). From the chemical analysis of total iron and the relative intensities of the three doublets, one can deduce that the paramagnetism of this sample is due to the presence of 2.09% of Fe^{2+} ions in the phyllosilicates (mainly in chlorite). Indeed pyrite has a very weak susceptibility (Serres 1953), negligible compared with the paramagnetic and even diamagnetic contributions. On the other hand the Curie constant, C, deduced from the curve in Fig. 3, corresponds to 2.06% of Fe^{2+}. The good agreement between magnetic and spectroscopic analyses shows that the separation of the paramagnetic contribution, using the magnetization measurements, is truly effective. In all the studied samples the susceptibility of the matrix is mainly due to paramagnetic iron in the phyllosilicates.

In the induced magnetization the ferromagnetic contribution is hidden by the paramagnetic one; this makes thermomagnetic studies unsuccessful in the identification of the ferromagnetic grains, as has been pointed out also by Lowrie & Heller (1982). The ferromagnetic

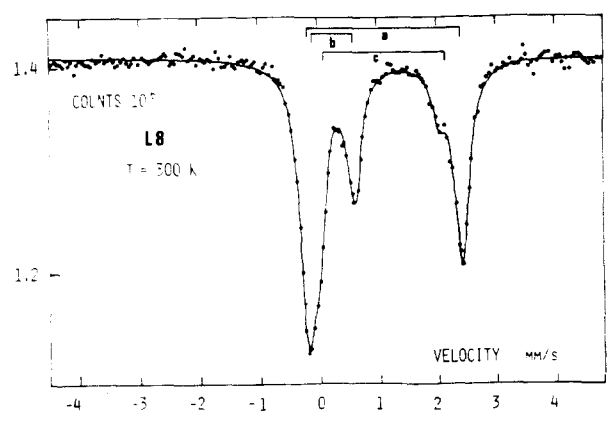

Fig. 4. Mössbauer spectrum of powdered sample L8 at 300 K. The solid line represents the best least-squares fit of the spectrum.

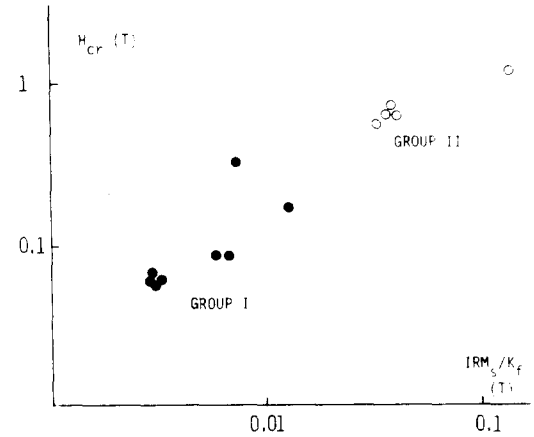

Fig. 5. Plot of the remanent coercive force, H_{cr}, against the ratio of IRM_s to K_f for all studied samples showing the separation in two groups (full and open circles).

contribution can be only studied through the properties of IRM. The acquisition curve of IRM permits the determination of the remanent coercive force H_{cr}. In Fig. 5 the coercive force of all studied samples is plotted against the ratio of IRM_s to K_f. This ratio takes into account the induced magnetic properties and seems to be an interesting parameter, coupled with H_{cr}, to differentiate the ferromagnetic grains according to their nature and grain size (see Hartstra 1982). This plot shows two groups of samples, with some intermediate ones. Group I is typical of a ferrimagnetic mineral and could correspond to fine-grained titanomagnetite according to the studies of Hartstra (1982). Group II corresponds to a mineral with a very high coercive force: in fact the IRM is not saturated even at 5 T. The stepwise thermal demagnetization of IRM_s shows for all samples of group I the same behaviour with maximum blocking temperatures around 520°C (Fig. 6). For group II samples a drastic decrease of IRM is observed between 20 and 80°C; together with the high value of H_{cr} this fact identifies poorly crystallized goethite due to weathering (Lowrie & Heller 1982). The abrupt increase of the susceptibility K_0 after heating over 350°C is linked to the dehydration of goethite into hematite, which is optically obvious. The breakdown of pyrite into magnetite probably occurs in all samples and leads to a general increase of K_0. In the samples containing goethite the value and behaviour of IRM_s after the thermal cleaning at 80°C is similar to those of group I samples. All these facts would indicate that in all the sites the original ferromagnetic mineral consists of fine-grained iron-rich titanomagnetite. Such grains have effectively been observed by microprobe analysis of a magnetic extract; but there are

Table 1. Mössbauer parameters of the three quadrupole doublets of the spectrum (Fig. 4). δ, Δ and Γ are respectively (in mm/s) the isomer shift relative to iron metal, the quadrupole splitting and the line-width at half height; I is the relative intensity in per cent

Doublet	δ	Δ	Γ	I	Assignment
a	1.12	2.61	0.30	53%	Chlorite Fe^{2+}
b	0.30	0.62	0.30	35%	Pyrite Fe^{2+}
c	1.10	2.18	0.40	12%	Muscovite Fe^{2+}

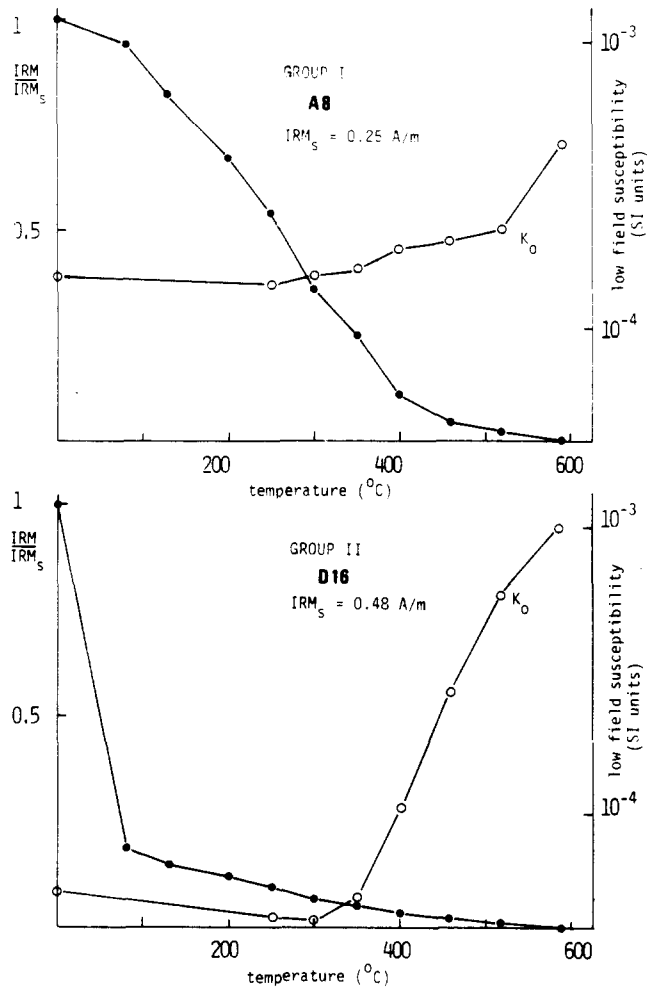

Fig. 6. Stepwise thermal demagnetization of IRM$_s$ and correlative change in the low-field susceptibility for group I and group II samples.

also some spherules of iron sulphides which could contain some pyrrhotite (Rochette 1983). Thus the presence of a mixture of titanomagnetite and pyrrhotite cannot be totally discarded.

The formation of goethite in weathered samples, traced by IRM properties, has also an effect on the matrix susceptibility K_l (Fig. 7). Indeed the conversion of the paramagnetic iron of phyllosilicates into the antiferromagnetic iron of goethite diminishes the value of K_l while the total iron content keeps roughly constant around 2.5%. Except for this weathering effect the value of K_l is more or less the same, around 130×10^{-6}, throughout the whole studied area. On the contrary the susceptibility of the ferromagnetic grains, K_f, shows an abrupt decrease when entering the epizone (sites H to L, Fig. 7). The presence of goethite has no visible effect on the value of K_f which is supposed to be only due to titano-magnetite. It seems that this mineral is partly destroyed by a metamorphic reaction occurring in the epizone.

The orientation of the principal axes

The directions of K_1, the maximum axis and K_3, the minimum axis of the low-field susceptibility ellipsoid are plotted and compared with the structural elements for the twelve sites in Fig. 8. In sites A and B where the directions are rather scattered due to the weak anisotropy degree, the K_3 directions lie close to the pole to bedding while the K_1 directions show a spread of orientations within the bedding plane. This would indicate a planar sedimentary fabric perhaps soon disturbed by tectonic deformation. In sites C, D, F and G a magnetic lineation (that is, a grouping of K_1 directions) is clearly defined and parallel to the bedding-cleavage intersection. As for the magnetic foliation it is still parallel to the bedding in site C while in the others a competition between the bedding and cleavage planes explains the directional scatter of K_3. In sites E, H, I, J and K the magnetic foliation is now well-defined and parallel to the cleavage plane while K_1 directions are widely scattered. In the Megève region (sites H, I and J) this scatter could be the result of the competition between the bedding-cleavage intersection and the transport lineation; meanwhile there is a slight tendency toward the transport lineation. This tendency is much clearer in site K. Finally in site L a clear magnetic lineation parallel to the transport lineation appears, while the magnetic foliation parallel to the cleavage is much less defined.

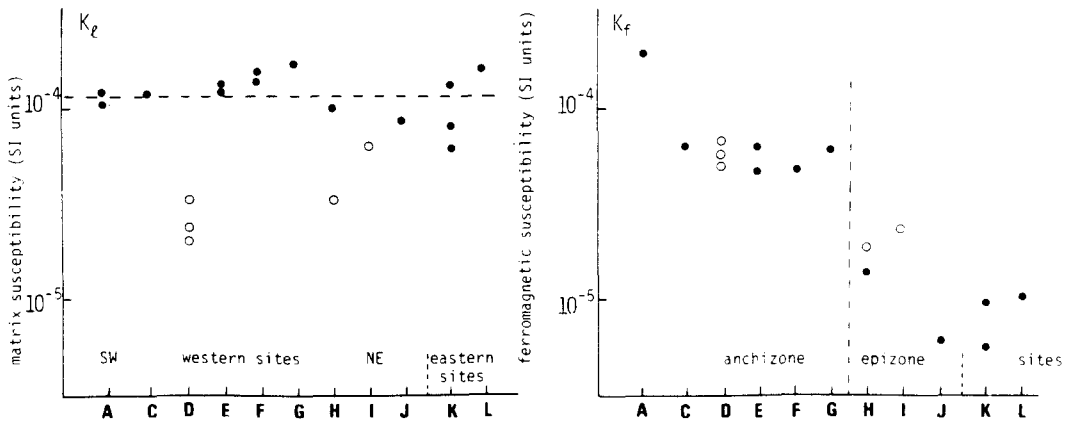

Fig. 7. Diagrams of the matrix and ferromagnetic susceptibilities, K_l *and* K_f, in selected samples of different sites classified according to increasing deformation and metamorphism. Open symbols correspond to the samples where IRM is mainly carried by goethite.

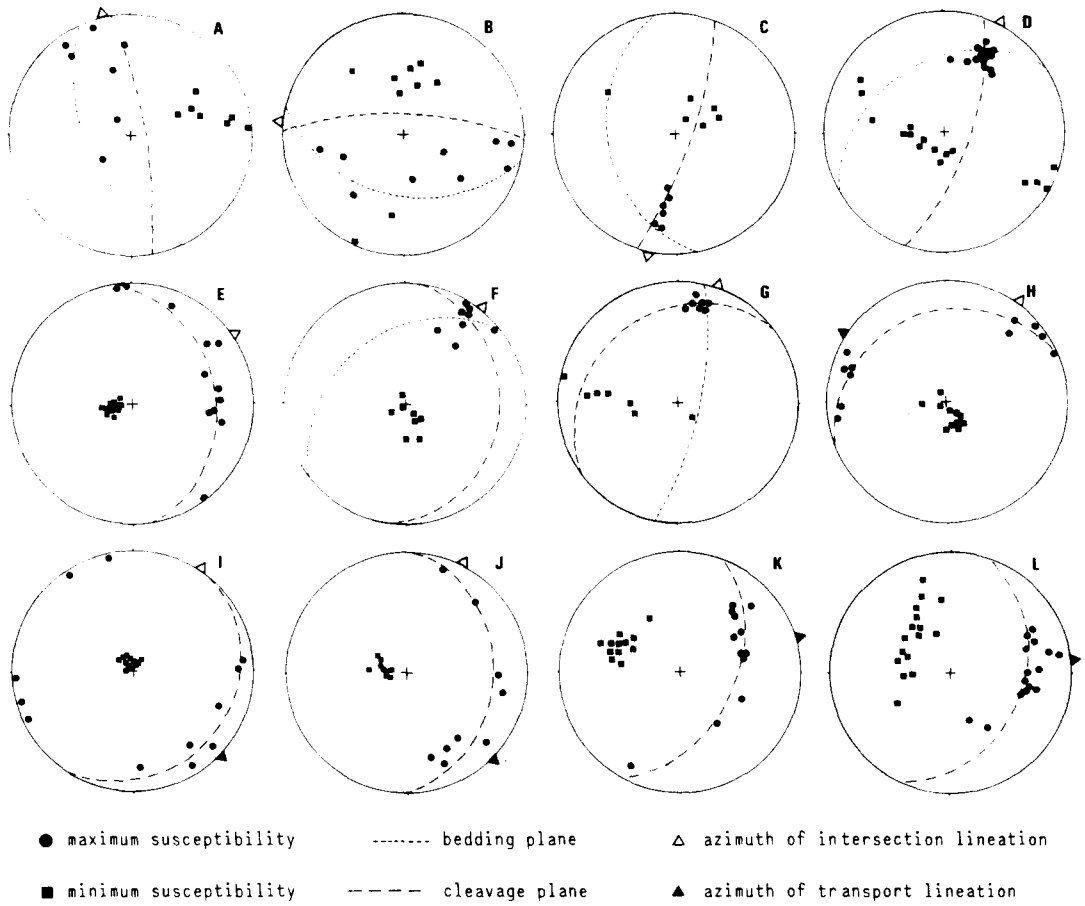

Fig. 8. Stereoplots of the maximum and minimum axes of the low-field susceptibility ellipsoid for the twelve sites (Fig. 1), compared with the structural elements. In several cases the bedding is not indicated because it is almost parallel to the cleavage. At site D a small fold has been sampled; the general bedding and the axial-plane cleavage are indicated.

The shape and intensity of the magnetic fabric

Arithmetical means of the shape parameter V and the anisotropy degree P have been calculated for each site (Fig. 9). The succession of the different planar and linear fabrics also appears when considering these two parameters: V is positive for a predominant planar fabric and negative for a predominant linear fabric; roughly speaking the anisotropy degree P increases with deformation.

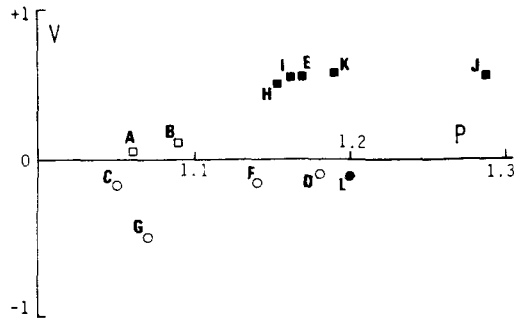

Fig. 9. Variation of the site mean-shape parameter, V, with the site mean-anisotropy degree, P, for the twelve sites, showing the different fabric types (Fig. 8). Circles correspond to prolate fabric and squares to oblate fabrics.

DISCUSSION

The qualitative agreement between the axes and shape of magnetic fabric and petrofabric is rather good in these rocks showing various fabric types. A similar trend was observed by Kligfield *et al.* (1981) in Permian red shales. However no direct quantitative correlation between strain and magnetic anisotropy could be drawn from the present data; indeed it has been shown that the low-field susceptibility has two main contributions: the paramagnetic one of phyllosilicates and the ferrimagnetic one of titanomagnetite. The within and between sites variability in their relative ratio due to lithology, metamorphism and weathering (see Fig. 7), results in a strain independant variation of the total magnetic anisotropy. With the present available data for K_f and K_l it is not possible to correct the low field anisotropy data for the effect of the matrix susceptibility.

Measurements of K_0 and K_l with the cryogenic magnetometer along the maximum and minimum axes of samples cut according to the petrofabric axes show that the origin of the total anisotropy is variable. The matrix susceptibility is almost isotropic in the sites with sedimentary or intersection fabric. But when the cleavage is well developed, the anisotropy degree of K_l becomes important, up to 1.22. This is due to a strong preferred orientation of phyllosilicates parallel to the

cleavage plane. Indeed phyllosilicates exhibit a maximum paramagnetic susceptibility within the silicate planes, as shown by Ballet (1979) and Ballet & Coey (1982), in particular for chlorite and muscovite. The contribution of the paramagnetism of phyllosilicates to the total anisotropy is important in sites E, H and I, and is almost the only one in sites J, K and L, as deduced from Fig. 7.

The anisotropy of the ferromagnetic contribution, which governs the total anisotropy in the less deformed sites is due to shape alignment of titanomagnetite grains. This alignment could be the result of individual grain rotation during continuous strain. But in the case of the tectonic fabrics, considering the importance of pressure-solution processes and the frequent occurrence of planar or linear clusters of opaque grains within solution planes, it is probably more realistic to assign the origin of anisotropy to the solution planes themselves, as stated by Borradaile & Tarling (1981) in a similar situation. In this model, magnetic interactions between titanomagnetite grains of an identical cluster would produce the overall anisotropy. If such a mechanism actually occurs, it rules out a quantitative correlation between strain and magnetic anisotropy in rocks where pressure-solution processes take place: no mathematical relation can arise from the addition of a discontinuous process and anisotropic magnetic interactions.

In this paper the influence of complex magnetic mineralogy and deformation mechanisms has been pointed out to emphasize the need for a close control of these two factors for successful investigations in the field of magnetic anisotropy.

Acknowledgements—Our colleagues of the Laboratoire Louis Néel and of the I.R.I.G.M. are gratefully acknowledged for their help and discussion. We would like to thank Dr C. Laj of the Centre des Faibles Radioactivités at the C.N.R.S., Gif sur Yvette, for allowing P.R. to use the magnetic anisotropy and remanence spinners in his laboratory, and Dr J. R. Regnard of the D.R.F., Centre d'Etudes Nucléaires de Grenoble, who has done the Mössbauer spectroscopy.

REFERENCES

Ballet, O. 1979. Fe^{2+} dans les silicates lamellaires. Etude magnétique et Mössbauer. Thesis, University of Grenoble.

Ballet, O. & Coey, J. M. D. 1982. Magnetic properties of sheet silicates; 2:1 layer minerals. *Phys. Chem. Minerals* **8**, 218–229.

Bernard, D., Gratier, J. P. & Pecher, A. 1977. Application de la microthermométrie des inclusions fluides des cristaux syn-cinématiques à un problème tectonique. *C.r. somm. Soc. géol. Fr.* **5**, 284–288.

Borradaile, G. J. & Tarling, D. H. 1981. The influence of deformation mechanisms on magnetic fabrics in weakly deformed rocks. *Tectonophysics* **77**, 151–168.

Carmichael, R. F. 1982. Magnetic properties of minerals and rocks. In: *Handbook of Physical Properties of Rocks, Vol. 2*. CRC Press, Boca Raton, Florida.

Coward, M. P. & Whalley, J. S. 1979. Texture and fabric studies across the Kishorn Nappe, near Kyle of Lochalsh, Western Scotland. *J. Struct. Geol.* **1**, 259–273.

Evans, B. J., Johnson, R. G., Senftle, F. E., Blaine Cecil, C. & Dulong, F. 1982. The 57 Fe Mössbauer parameters of pyrite and marcasite with different provenances. *Geochim. cosmochim. Acta* **46**, 205–215.

Gratier, J. P. 1982. Approche expérimentale et naturelle de la déformation des roches par dissolution–cristallisation, avec transfert de matière. *Bull. Mineral.* **105**, 291–300.

Gratier, J. P. & Vialon, P. 1980. Deformation pattern in a heterogeneous material: folded and cleaved sedimentary cover immediately overlying a crystalline basement (Oisans, French Alps). *Tectonophysics* **65**, 151–180.

Hartstra, R. L. 1982. Grain-size dependence of initial susceptibility and saturation magnetization-related parameters of four natural magnetites in the PSD–MD range. *Geophys. J.R. astr. Soc.* **71**, 477–495.

Heller-Kallai, L. & Rozenson, I. 1981. The use of Mössbauer spectroscopy of iron in clay mineralogy. *Phys. Chem. Minerals* **7**, 223–238.

Hrouda, F. 1982. Magnetic anisotropy of rocks and its application in geology and geophysics. *Geophys. Surveys* **5**, 37–82.

Jelinek, V. 1981. Characterization of magnetic fabric of rocks. *Tectonophysics* **79**, 563–567.

Kligfield, R., Owens, W. H. & Lowrie, W. 1981. Magnetic susceptibility anisotropy, strain, and progressive deformation in Permian sediments from the Maritime Alps. *Earth Planet. Sci. Lett.* **55**, 181–189.

Lowrie, W. & Heller, F. 1982. Magnetic properties of marine limestones. *Rev. Geophys. Space Phys.* **20**, 171–192.

Owens, W. H. & Bamford, D. 1976. Magnetic, seismic, and other anisotropic properties of rock fabrics. *Phil. Trans. R. Soc.* **A283**, 55–68.

Pijolat, B., Gay, M., Gratier, J. P. & Vialon, P. 1981. Les variations des valeurs de la déformation dans un système de plis par cisaillement. *Revue Géogr. phys. Géol. dyn.* **23**, 177–195.

Ramsay, J. G. 1963. Stratigraphy, structure and metamorphism in the Western Alps. *Proc. geol. Ass.* **74**, 357–391.

Ramsay, J. G. 1982. Variations in linear and planar fabrics in the western Helvetic nappes, Switzerland. *Mitt. geol. Inst. ETH Univ. Zürich* **239a**, 230–232.

Rochette, P. 1983. Propriétés magnétiques et déformations de roches sédimentaires alpines. Thesis, University of Grenoble.

Rochette, P., Fillion, G., Mollard, P. & Vergne, R. 1983. Utilisation d'un magnétomètre à effet Josephson pour l'analyse de l'anisotropie magnétique des roches. *C.r. hebd. Séanc. Acad. Sci., Paris* **296**, 557–559.

Serres, A. 1953. Sur quelques composés du cobalt et du fer à paramagnétisme très faible et constant. *J. Phys. Rad.* **14**, 689–690.

Zwart, H. J. 1973. *Metamorphic map of Europe: Sheet* 17. Leiden and UNESCO, Paris.